Heat Transfer Characteristics of a Radial Jet Reattachment Flame

J. W. Mohr

J. Seyed-Yagoobi

R. H. Page

Drying Research Center,
Department of Mechanical Engineering,
Texas A&M University,
College Station, TX 77843-3123

A Radial Jet Reattachment Combustion (RJRC) nozzle forces primary combustion air to exit radially from the combustion nozzle and to mix with gaseous fuel in a highly turbulent recirculation region generated between the combustion nozzle and impingement surface. High convective heat transfer properties and improved fuel/air mixing characterize this external mixing combustor for use in impingement flame heating processes. To understand the heat transfer characteristics of this new innovative practical RJRC nozzle, statistical design and analysis of experiments was utilized. A regression model was developed which allowed for determination of the total heat transfer to the impingement surface as well as the NO_x emission index over a wide variety of operating conditions. In addition, spatially resolved flame temperatures and impingement surface temperature and heat flux profiles enabled determination of the extent of the combustion process with regards to the impingement surface. Specifically, the relative sizes of the reaction envelope, high temperature reaction zone, and low temperature recirculation zone were all determined. At the impingement surface in the reattachment zone very high local heat flux values were measured. This study provides the first detailed local heat transfer characteristics for the RJRC nozzle.

Introduction

Flame jet impingement is an often utilized method for heat treating processes involving, for example, metals and glass, and it offers several advantages over traditional radiative furnaces. First, since convection heat transfer is significant, very rapid and intense heating is possible. Secondly, direct transfer of the energy from combustion to the surface eliminates the need for radiative refractory materials. Lastly, the process becomes more fuel efficient with the elimination of heat transfer losses associated with the heat-up of radiative furnaces.

A review by Viskanta (1993) of the limited number of investigations involving single round impinging in-line jet (ILJ) flames showed that the major disadvantage of impinging flame jets was the nonuniform surface heat flux and temperature distribution near the jet stagnation point. A novel approach to the solution of these problems involved changing the aerodynamics of the impinging flame jet through an application of Radial Jet Reattachment (RJR) nozzles (Page et al., 1989). Extension of the RJR concept for flame jet impingement applications resulted in a Radial Jet Reattachment Combustion (RJRC) nozzle (Habetz et al., 1994; Mohr et al., 1995, 1996). A typical air flow pattern for either a nonreacting RJR nozzle or a reacting RJRC nozzle is depicted in Fig. 1. The internal air stream of the RJR or RJRC nozzle forces air to exit the nozzle in an outward radial direction. Viscous mixing and mass entrainment causes the exiting air jet to turn toward the impingement surface, where it impinges in a highly turbulent reattachment ring centered about the nozzle. Previous studies have shown that this reattachment region has very high convective heat and mass transport properties (Page et al., 1989). The size of the ring-shaped stagnation region is dependent upon the air exit velocity (V), the air exit angle (θ), and the nozzle-to-plate spacing (X_p/R_o). The air exit velocity at a given flow rate is controlled by the gap width (b/R_o) between the large circular disk and the end of the air pipe. Within the reattachment ring, a subatmospheric pressure recirculation region is created. As shown in Fig. 1, a RJRC nozzle is created from a typical RJR nozzle by introducing gaseous fuel radially into the recirculation region, ensuring that the fuel does not directly impinge upon the surface. The net force exerted on the impingement surface by an RJRC nozzle can be negative, null, or positive depending on the air exit angle of the nozzle. An air exit angle (θ) of 10 deg was machined into the upper disk of the RJRC nozzle, so a slight positive force upon the impingement surface in the reattachment ring was expected.

The present work is a follow-up of the Mohr et al.'s (1996) work, where the combustion characteristics of a large prototype RJRC nozzle were presented. In that work, the RJRC concept was compared to a standard in-line jet (ILJ) flame impingement nozzle. The RJRC nozzle showed slightly higher overall heat transfer to the impingement surface than the ILJ nozzle, with both nozzles operating over a large range of fuel equivalence ratios. In addition, the RJRC nozzle produced a circumferentially symmetric surface temperature distribution and exerted very little force upon the impingement surface. Compared with the RJRC nozzle, the ILJ nozzle produced a nonsymmetric surface temperature distribution and the maximum surface pressure with combustion was more than six times the RJRC nozzle surface pressure. Combustion specie data obtained from a single radial location for the two nozzles revealed lower levels of carbon monoxide and NO_x for the RJRC nozzle. Since this study was based on overall global heat transfer and combustion measurements, no localized data on flame temperature, surface heat flux, or combustion specie concentrations were obtained.

The present work adds to the basic understanding of the RJRC concept through an investigation of a smaller practical RJRC nozzle more suitable for possible implementation into an industrial process. Statistically designed experiments are utilized, and the data from these experiments are used to determine a regression model by which the heat transfer and NO_x formation characteristics of the RJRC nozzle can be predicted. In addition, localized heat transfer data (flame temperatures, impingement surface temperature profile, and impingement surface heat flux distribution) are determined for the RJRC nozzle

Contributed by the Heat Transfer Division for publication in the JOURNAL OF HEAT TRANSFER. Manuscript received by the Heat Transfer Division May 21, 1996; revision received November 14, 1996; Keywords: Combustion, Fire/Flames, Furnaces & Combustors. Associate Technical Editor: S. H. Chan.

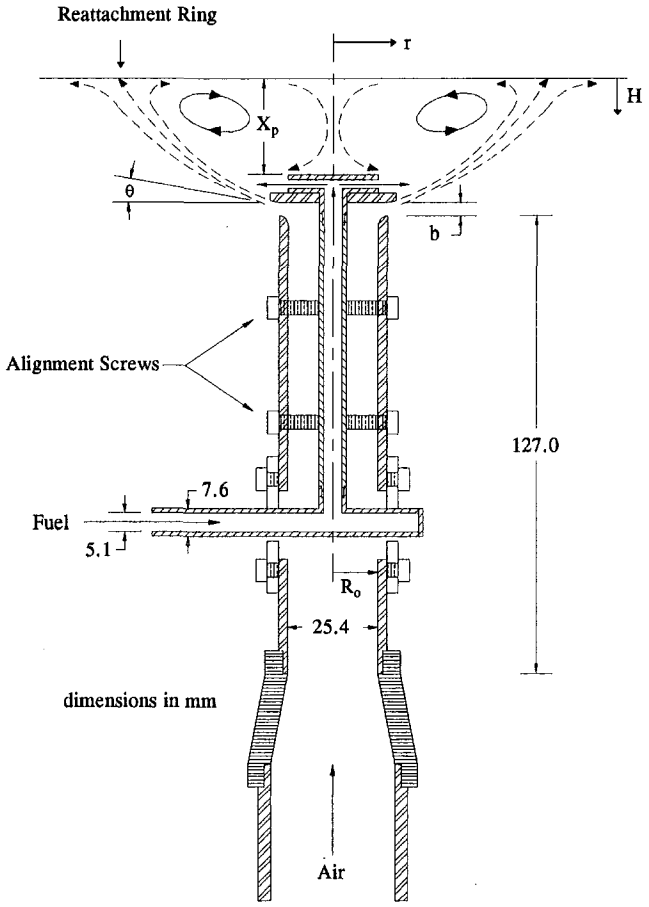

Fig. 1 RJRC nozzle and representative flow field

operating at an ideal condition. These data are utilized to determine the relative sizes of the RJRC reaction, recirculation, and reattachment zones.

Experimental Apparatus and Procedure

The combustion jet impingement facility, consisting of a support structure, combustion nozzle, and impingement surface is shown schematically in Fig. 2. The flame impingement surface is a 6.35 mm thick, 0.836 m^2 copper plate, which is uniformly cooled by a water heat exchanger in contact with the backside of the copper plate. The total heat transfer rate to the surface on an integral basis was determined by measuring the cooling water flow rate and its change in temperature, with the cooling water flow rate held constant at 22.7 liters/min. All measurements were obtained under steady-state, wherein the exit temperature of the cooling water ceased to change following a change in burner operating conditions. The change in temperature (typically about 4.0°C) was measured using thermistor thermometers with an accuracy of ±0.2°C. In order to provide a measure of the efficiency of the combustion process, the rate of heat transfer (q) to the surface was normalized by the rate of energy available from the fuel input to the system (q_f). The resulting variable was designated as the heat transfer ratio, R_t. The total available energy rate was determined by multiplying the heating value of the working gas by its flow rate. The working gas in this study was utility natural gas (90 percent methane) having a heating value of 61,594 kJ/kg.

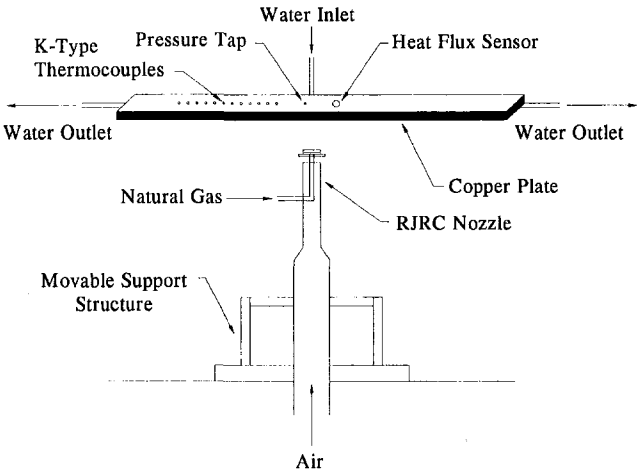

Fig. 2 Combustion jet impingement facility

Impingement surface local heat flux was measured with a single Vatell Corporation factory calibrated HFM-2 heat flux sensor mounted flush with the front side of the impingement surface as shown in Fig. 2. This 0.2 mm wide line sensor is mounted on a 25.4 mm OD, 6.35 mm thick aluminum nitride substrate. The depth of the sensing pattern is 2 μm, making it nearly invisible to any boundary layer flow across the sensor. The HFM-2 sensor is cooled from the backside in an identical manner as the rest of the copper plate. Measurement of the heat flux profile along the impingement surface was possible by moving the RJRC flame horizontally. Each local heat flux measurement was the average of 14,336 data points sampled at a rate of 500 samples/second. Flame temperatures were measured using a 50 μm diameter Type S bare wire thermocouple with an accuracy of ±1.5°C. The measured flame temperatures were corrected for convection and radiation effects according to Bradley and Matthews (1968) and Boyer (1990). Reported mean temperatures represented the average of 12,300 temperature readings recorded at a rate of 2000 samples/second.

Nomenclature

b/R_o = RJR nozzle exit gap width, dimensionless
D_f = fuel pipe inside diameter = 5.1 mm
ENO_x = NO_x emission index, (g NO_x/kg fuel)
H = distance measured from impingement surface, mm
ILJ = in-line jet
MW = molecular weight, g/mol
n = average number of carbon atoms in fuel structure per mole of fuel = 1.05
q = plate heat transfer rate, kW
q_f = fuel heating capability, kW
q'' = local heat flux, W/m^2
q''_{avg} = area averaged heat flux, W/m^2
r = radial location, mm
R_o = air supply pipe inside radius = 12.7 mm
Re = fuel Reynolds number (based on D_f), dimensionless
RJR = radial jet reattachment
RJRC = radial jet reattachment combustion
R_t = heat transfer ratio = q/q_f, percent
V = air exit velocity, m/sec
X_p/R_o = nozzle-to-plate spacing, dimensionless
W = dependent variable
[ ] = concentration, mol/cm^3
θ = air exit angle = 10 deg
Φ = fuel equivalence ratio = (Fuel/Air Ratio)$_{actual}$/(Fuel/Air Ratio)$_{stoichiometric}$

The near-surface temperatures of the impingement surface were measured with K-type thermocouples (20 AWG) with a calibrated accuracy of ±0.5°C. Twelve thermocouples spaced 25.4 mm apart were silver-soldered to the bottom of holes drilled from the rear of the copper plate to within 1.5 mm of the impingement side. A single pressure tap was drilled through the copper plate near the center of the copper plate, as shown in Fig. 2. Surface pressure profiles were possible by moving the support structure, i.e., flame, horizontally while the surface remained stationary. A variable reluctance differential pressure transducer, with an accuracy of ±0.25 percent full scale, was connected to the pressure tap by flexible tubing. The average local gage pressure was calculated from 2048 samples taken at a rate of 200 samples/second.

Combustion specie concentrations were collected from the flame region through a 4.0 mm ID, 6.0 mm OD quartz isokinetic gas sampling probe as outlined by Mohr (1996). The overall emission index of NO_x (ENO_x) was determined from the measured quantities of CO_2 and NO_x ($NO + NO_2$), respectively, and is shown in Eq. 1.

$$ENO_x = \frac{n[NO_x]MW_{NO_2}1000}{[CO_2]MW_{fuel}} \quad (1)$$

This index expresses the grams of NO_x produced per kilogram of fuel burned and best characterizes the emissions from open system diffusion flames (Turns and Lovett, 1989; Junus et al., 1994; Røkke et al., 1994). A complete emissions mapping (Mohr, 1996) with respect to r/R_o at a given value of H/R_o showed the NO_x emission index to be invariant with r/R_o and H/R_o. Therefore, the statistical model emissions data were obtained at $H/R_o = 0.8$ at a nondimensional radial distance of $r/R_o = 36$, just prior to the point where the combustion gases were drawn into the exhaust duct.

Error Analysis. Using the method of Kline and McClintock (1953), the uncertainty in heat transfer ratio was 10.2 percent, while the uncertainty in fuel equivalence ratio (based on the metered air and fuel flow rates) was 4.0 percent. The minimum and maximum uncertainties in the surface heat flux profile were 1.4 and 11.4 percent, respectively. The impingement surface pressure coefficient profile had minimum and maximum uncertainties of 2.6 and 12.8 percent, respectively. The minimum and maximum uncertainties in the surface temperature measurements were 3.0 and 7.4 percent, while the flame temperatures showed an uncertainty range of 0.25–4.0 percent.

Several runs at identical operating conditions were conducted and averaged. The standard deviation of the heat transfer ratio was 1.37 percent. Within the stagnation region, the minimum and maximum standard deviations in local heat flux values were 2.3 and 15.9 percent of the reported mean heat flux values. Repeatability data for the plate surface temperature measurements showed minimum and maximum standard deviations to be 0.7 and 2.8 percent, respectively. Repeatability data for the combustion gas concentrations yielded standard deviations of 0.53, 1.45, 14.6, and 6.0 percent of the mean values for O_2, CO_2, CO, and NO_x measurements, respectively.

RJRC Flame Characterization

In combustion systems utilizing natural gas, a compromise exists between maximizing heat transfer and minimizing pollution formation. Minimum levels of CO are present when flame temperatures are high, since the conversion of CO to CO_2 is enhanced by higher temperatures. However, higher temperatures also promote the formation of thermal NO_x compounds, so one must sacrifice some level of heat transfer (i.e. flame temperature) to attain the desired low levels of NO_x compounds.

Statistical Design. Based on previous studies (Habetz et al., 1994), four major factors affect the heat transfer and pollution formation processes for the RJRC combustion nozzle: (1) fuel Reynolds number (Re), (2) fuel equivalence ratio (Φ), (3) nozzle air exit width (b/R_o), and (4) nozzle-to-plate spacing (X_p/R_o). The primary air flow rate is built into the definition of Φ. Habetz et al. (1994) conducted limited investigations of the effects of each of these factors, but those experiments were conducted by setting all but one of the variables at a constant value and testing over a range of the remaining variable. Utilizing such an experimental method requires a large number of experimental runs and does not give information about the possible interaction between factors. Attempts to use nondimensional analysis in constructing an empirical heat transfer correlation for RJRC performance were not completely successful (Habetz et al., 1994), and there exists great difficulty in numerically modeling the highly turbulent reacting system. Therefore, a statistical model was used to bridge the gap between purely empirical and purely analytical models through a relatively small number of experimental runs. The power of using designed experiments is that one can construct a statistical model that is easy to use and yields valuable performance data useful to a process operator or designer.

Previous investigations (Mohr et al., 1996) showed nonlinear trends in heat transfer and pollution formation as functions of fuel equivalence ratio and fuel Reynolds number, so a traditional 2^k (k factors at 2 different levels) factorial experimental design would be inappropriate in modeling any nonlinear responses. A third level would be required to pick up any quadratic or higher order nonlinear behavior. The difficulty in adding a third level is that 3^4 runs would be required to fully investigate four experimental factors at three different levels. In order to reduce the total number of experimental runs from 81 to 27, a Box-Behnken (Box and Behnken, 1960) experimental design method for four factors was used. This design is similar to a four factor Central Composite Design (Hogg and Ledolter, 1992), but with six fewer experimental runs. One other advantage of a Box-Behnken design is that it lends itself well to fitting higher order quantitative models to experimental data.

Statistical Models. The levels of each of the four main factors were chosen based on several criteria. Lean blow-out data set the lower limits on the fuel Reynolds number (Re) and Φ at 5253 and 1.0, respectively. The upper limits of these two variables were determined based on the limitations of the small RJRC nozzle to safely operate. Within these limits, each variable (Re and Φ) could be varied independently of each other and still maintain a stable flame. The values of nozzle-to-plate spacing, X_p/R_o, were chosen in order to maintain flame stability at the different levels of the other variables. The range of exit gap width, b/R_o, represents the minimum and maximum openings possible with the current RJRC nozzle construction. The levels of each of the four factors are listed in Table 1. Note that the intermediate level of each variable is determined from the arithmetic average of the upper and lower limits, respectively.

Based on the data obtained from the 27 runs in the Box-Behnken design, a second order regression analysis was applied using commercially available statistical software. The resulting

Table 1 Box-Behnken design factor levels

Factor	Low Level	Medium Level	High Level
Φ	1.0	1.5	2.0
Re	5253	8855	12456
X_p/R_o	0.79	1.18	1.57
b/R_o	0.12	0.26	0.40

regression equation for a particular dependent variable, W (R_t or ENO_x), was constructed according to the format of Eq. 2, wherein the first order, interaction, and second order terms are all considered.

$$W = C_1 + C_2\Phi + C_3(X_p/R_o) + C_4 b/R_o + C_5\,\mathrm{Re} + C_6\Phi^2 + C_7(\Phi)(X_p/R_o) + C_8(\Phi)(b/R_o) + C_9(\Phi)(\mathrm{Re}) + C_{10}(X_p/R_o)^2 + C_{11}(X_p/R_o)(b/R_o) + C_{12}(X_p/R_o)(\mathrm{Re}) + C_{13}(b/R_o)^2 + C_{14}(b/R_o)(\mathrm{Re}) + C_{15}\,\mathrm{Re}^2 \quad (2)$$

Statistical analysis revealed that not all of the coefficients in Eq. 2 were statistically significant at a 95 percent confidence level, so it was possible to reduce the number of terms in Eq. 2 considerably. Equations 3 and 4 show the resulting expressions for R_t, and ENO_x, respectively, as well as the correlation coefficients for each expression. The high correlation coefficients (R^2) demonstrate that the models are accurately describing the variability in the data.

$$R_t(\text{percent}) = -86.4 + 51.8\Phi + 194 b/R_o + .00927\,\mathrm{Re} - 11.2\Phi^2 - 266(b/R_o)^2 - 4.8 \times 10^{-7}\,\mathrm{Re}^2 \qquad R^2 = 95.9 \text{ percent} \quad (3)$$

$$ENO_x = 1.36 - 0.448\Phi - 1.87 b/R_o - 1.07 \times 10^{-4}\,\mathrm{Re} + 0.969(\Phi)(b/R_o) + 6.1 \times 10^{-5}(\Phi)(\mathrm{Re}) + 1.73 \times 10^{-4}(b/R_o)(\mathrm{Re}) \qquad R^2 = 93.4 \text{ percent} \quad (4)$$

The statistical analysis revealed that the heat transfer ratio, R_t, was dependent upon the first and second order terms, and independent of the interaction among variables. Some interaction terms were important for ENO_x, while the second order terms were not important. For both response variables, though, the effect of nozzle-to-plate spacing (X_p/R_o) was statistically insignificant. This finding is in contrast to studies with ILJ flame jets where the nozzle-to-plate spacing greatly affected the impingement surface heat transfer (Baukal and Gebhart, 1995a, 1995b; Viskanta, 1993; Rigby and Webb, 1995). Additional experimental data within the range of parameters were obtained in order to test the ability of the model to predict heat transfer and pollution formation with the RJRC nozzle. The differences between all experimental data and the model were less than 7.6 and 11.5 percent for R_t and ENO_x values, respectively. These statistical methods allow for the development of a powerful, yet simple equation which accurately predicts the RJRC nozzle performance.

Heat transfer results from the statistical model are shown in Fig. 3 and indicate that as the air exit gap width, b/R_o, increases, percent heat transfer to the impingement surface increases. One reason for this behavior is that a larger value of b/R_o results in a slower air exit velocity, allowing more time for the fuel and air to fully mix and react. Also, the slower air jet velocity creates a longer residence time for the reacting gasses flowing along the surface following impingement. For larger values of b/R_o, the amount of heat transfer to the impingement surface was quite significant, where up to 50 percent of the available fuel energy was transferred to the impingement surface. The quadratic trend with respect to Re suggests that R_t can be increased by increasing the amount of fuel supplied to the system up to Re = 9656, after which an increase in Re causes a decrease in R_t. A continual increase in Re will lead to an eventual decrease in R_t due the fixed size of the impingement surface. For a constant value of Re, the fuel equivalence ratio was increased by decreasing the air flow rate, and hence, the air velocity. Figure 3 shows that percent heat transfer increases with increasing Φ at a constant value of Re. The lower air flow velocities associated with higher Φ results in the same effect on R_t as increasing b/R_o, as discussed above. Finally, these values of

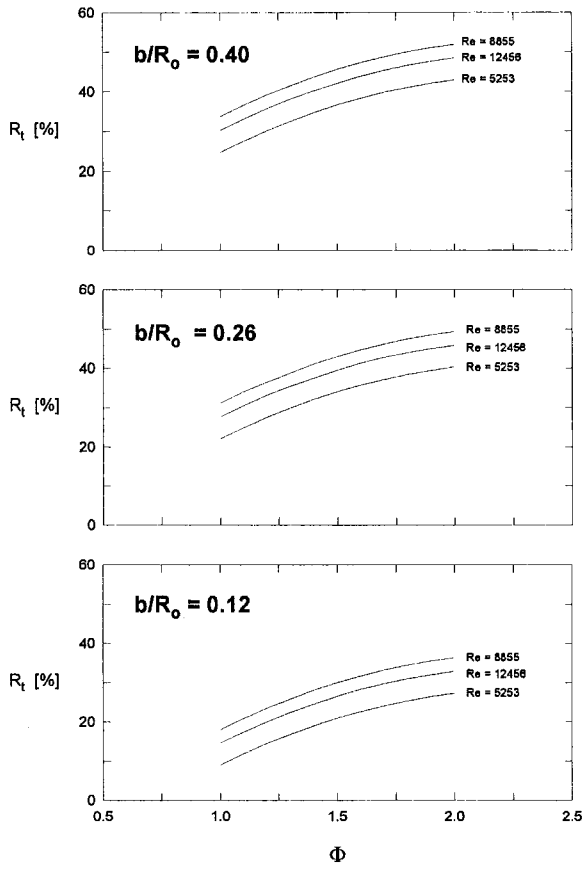

Fig. 3 Percent heat transfer calculated from regression model as a function of Re, Φ, and b/R_o

overall heat transfer compare quite well with other flame jet impingement studies such as Rigby and Webb (1995).

Ideal Condition Results

A procedure outlined by Mohr (1996) was utilized to determine the ideal operating conditions of the RJRC nozzle in terms of maximizing heat transfer and minimizing NO_x emissions. The results of that procedure yielded the following ideal operating conditions: Re = 8855, Φ = 1.0, and b/R_o = 0.29. Since the nozzle-to-plate spacing, X_p/R_o, was not a significant factor in either the heat transfer or ENO_x considerations, the mid-range value of X_p/R_o = 1.18 was selected for further testing. The following results and discussion correspond to the RJRC nozzle operating under these ideal operating conditions.

Flame Temperatures. Figure 4 shows the corrected temperatures for the RJRC flame. These six flame temperature profiles were obtained with the thermocouple probe held at six fixed distances from the impingement surface. The support structure (i.e., the flame) was moved horizontally, corresponding to radial measurement with respect to the flame. Due to the symmetry of the RJRC flame (Mohr et al., 1996), radial measurements were obtained from only one circumferential location. The radial flame temperature profiles for H/R_o = 0.4 and 0.8 were able to reach completely to the nozzle center-line, while the minimum radius for the other profiles was limited by the outer radius of the RJRC nozzle. With the RJRC nozzle, the maximum flame temperature at H/R_o = 0.4 was approximately twice that of the flame centerline temperature. A round flame jet for a methane/air mixture at a fuel Reynolds number of 7000 also resulted in a centerline flame temperature which was about half the maximum temperature (Milson and Chigier, 1973). The nozzle-to-plate spacing used with their round flame

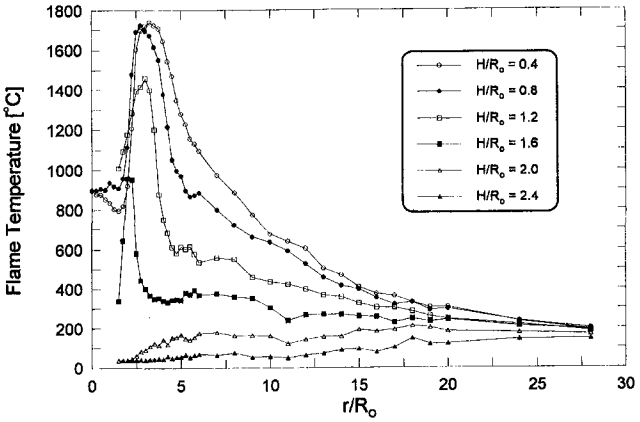

Fig. 4 RJRC flame temperatures at Re = 8855, Φ = 1.0, X_p/R_o = 1.18, b/R_o = 0.29

was 8.5 times larger than the nozzle-to-plate spacing used with the RJRC nozzle. Because of the cool central core of unreacted fuel present in round flame jets, a larger reaction zone (larger X_p/R_o) is required compared with the RJRC nozzle to achieve the same flame temperature at the nozzle centerline. The recirculation region at the centerline of the RJRC nozzle distributes the fuel and air more uniformly, allowing combustion to take place at the nozzle centerline without having to increase the size of the reaction zone by increasing the nozzle-to-plate spacing. The maximum measured flame temperature of Milson and Chigier's (1973) premixed flame was less than 2.0 percent higher than the maximum temperature measured at H/R_o = 0.4 in the present study. This result suggests that this partially premixed RJRC nozzle is operating essentially as a premixed burner.

The location of the reattachment ring is manifested by the steep gradients on both sides of the maximum flame temperatures for profiles where $H/R_o \leq 1.6$. It can be seen that the peak temperature moves radially outward with decreasing H/R_o, due to expansion of the air jet as it leaves the RJRC nozzle. This air jet expansion creates a larger oxygen-rich reaction zone in which combustion can occur, causing the radial width of the reaction zone to increase with decreasing H/R_o. For $H/R_o > 1.6$, the low temperatures indicate that no combustion is occurring, and suggest that the reaction zone is limited to $H/R_o \leq 1.6$. The change in slopes of the flame temperature profiles suggests that the combustion process is nearly complete at $r/R_o \approx 10$.

Surface Heat Flux. The impingement surface local heat flux and the area averaged heat flux defined by Eq. (5) as functions of radial location are shown in Fig. 5.

$$q''_{\text{avg}} = \frac{2\pi \int_0^{r/R_o} q''[r/R_o]d[r/R_o]}{\pi[r/R_o]^2} \qquad (5)$$

Also shown in Fig. 5 is the flame temperature profile for H/R_o = 0.4 and the impingement surface temperature distribution. The shape of the local heat flux profile, very closely mirrors the flame temperature profile with the exception that the maximum flame temperature occurs at a slightly smaller radial location than the maximum heat flux. This small difference in radial location is possibly due to the fact that the flame temperature was measured 5 mm from the impingement surface.

The data from Fig. 5 are extremely important. First, the high heat flux ($\approx$140 kW/m^2) within the reattachment region under the given operating conditions shows that very intense heating is possible with the RJRC nozzle. Even higher local heat flux values would be possible if one were to increase the fuel flow rate. The average heat flux profile calculated from Eq. 1 shows a significant drop beyond $r/R_o \approx 10$. This area-averaged heat flux profile is important when considering the optimal spacing between nozzles in an array configuration. The integrated local heat flux values calculated from Eq. 6 were compared to the overall heat transfer to the impingement surface, measured by the sensible heat gain of the cooling water.

$$q = 2\pi \int_0^{r/R_o=28} q''[r/R_o]d[r/R_o] \qquad (6)$$

This integrated heat transfer rate was 13 percent lower than the measured overall heat transfer rate. These differences can be attributed to the fact that the heat flux data were possible to be measured up to r/R_o = 28, whereas edge of the water-cooled impingement surface is located at r/R_o = 36. In fact, when the slope of the local heat flux profile is extrapolated out to the edge of the impingement surface (r/R_o = 36), the difference in the integrated and measured heat transfer rates is less than ten percent.

RJRC Flame Map. The characteristics of the RJRC flame have been mapped by combining the data from Figs. 4 and 5 with surface pressure and combustion specie data (Mohr, 1996) for the RJRC nozzle operating under same the ideal conditions. These data are plotted in Fig. 6, where all the nondimensional terms are in relative proportion to each other and the RJRC nozzle. Several distinct features of the RJRC flame are contained within Fig. 6. The reaction envelope, where the gas temperatures are all above 540°C, is located within the boundary of the shaded regions. Glassman (1987) reports that the spontaneous ignition temperature of a methane/air mixture is 540°C. Since the natural gas fuel utilized in this study is over 90 percent methane, it is reasonable to assume that its ignition temperature will be close to the ignition temperature of methane. Hence, any region at or above 540°C is likely to contain reacting combustion gases. It is important to point out the gap between the shaded region and the impingement surface ($0 < H/R_o < 0.4$). No flame temperature measurements were obtained in this region due to spatial limitations and concern in damaging the fine wire thermocouple probe. The same explanation applies to the gap between the shaded region and the top of the RJRC nozzle for $0 < r/R_o < 0.75$.

The main high temperature reaction zone occurs along the boundary of the moving primary air as it exits the RJRC nozzle and contacts the fuel stream. The higher mass flow rate of air

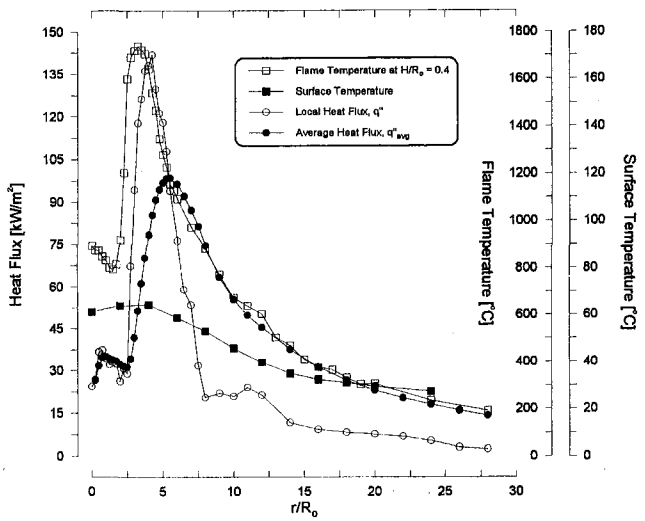

Fig. 5 Impingement surface heat flux and temperature distributions for the RJRC flame operating at Re = 8855, Φ = 1.0, X_p/R_o = 1.18, b/R_o = 0.29; flame temperatures measured at H/R_o = 0.4

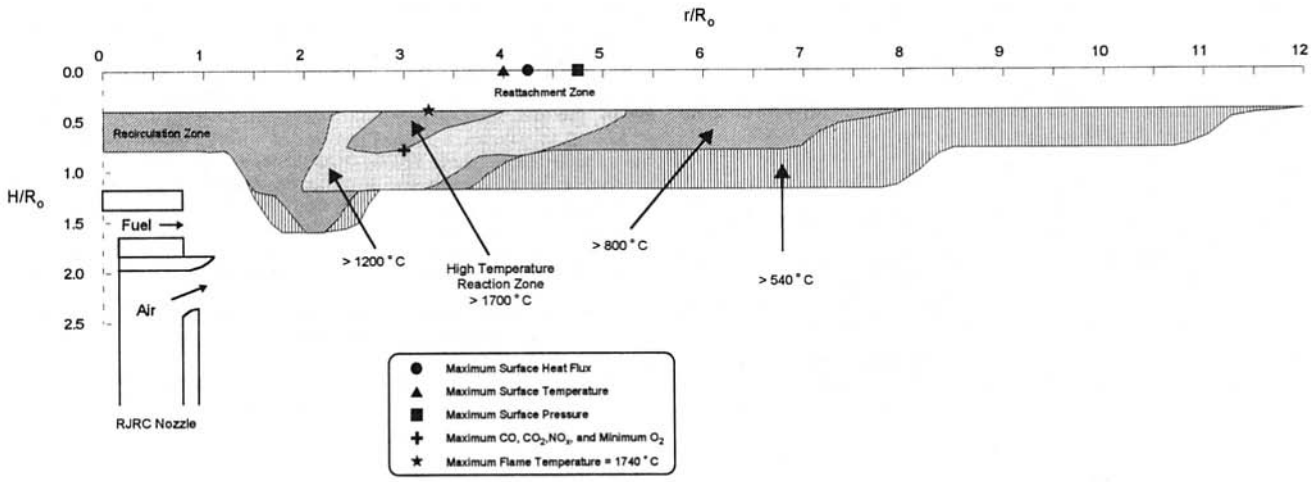

Fig. 6 RJRC flame map for the flame operating at Re = 8855, $\Phi = 1.0$, $X_p/R_o = 1.18$, $b/R_o = 0.29$

relative to the fuel forms the outer boundary of the reaction zone and directs the flame jet toward the impingement surface. As fuel and air react in the small zone between the fuel and air streams, the very high temperature (>1700°C) reaction zone forms over the distance $2.5 < r/R_o < 4.0$ for $0.4 < H/R_o < 0.8$ (see also Fig. 4). The combustion specie profiles (Mohr, 1996) confirmed the location of this high temperature reaction zone. The maximum concentration of CO, CO_2, and NO_x, as well as the minimum concentration of O_2, were all located at a single location in the horizontal plane at $H/R_o = 0.8$, namely $r/R_o = 3.0$. At this location, the high temperatures promoted near-stoichiometric combustion concentrations of CO_2 and O_2, respectively. A lower temperature (>1200°C) reaction zone is also present over the distance $2.00 < r/R_o < 5.25$. Except for a small region in the vicinity of $1.50 < r/R_o < 2.75$, the combustion specie profiles at $H/R_o \geq 1.2$ revealed very little chemical reactions, as also shown by the low (<540°C) flame temperatures in Fig. 6.

The relatively low temperature recirculation zone is located between the nozzle and the impingement surface. This region is identified by the fact that the temperatures were at or above 800°C but less than 1200°C. The reattachment zone on the impingement surface is clearly marked by the maximum values of surface temperature, surface pressure, and surface heat flux. Note that the width of the relatively thin reattachment zone is approximately 0.75 r/R_o, corresponding to 9.5 mm. As discussed above with regard to flame temperatures, the spreading of the flame jet prior to and following reattachment is shown in Fig. 6, as evidenced by the presence of the reaction envelope at radii both smaller and larger than the radial location of the reattachment zone.

Energy Balance. Energy from the RJRC flame is either transferred to the impingement surface, convected out of the system with the spent combustion products, or radiated to the surroundings. The magnitude of each of these losses was determined by Mohr (1996) for the RJRC nozzle operating under the same ideal condition as discussed previously. The results showed that 70 ± 8.5 percent of the fuel input energy was convected out of the impingement system in the form of hot combustion gases. The ±8.5 percent deviation in the convected energy value is a result of the approximate 12.0 percent overall uncertainty of the convected energy measurements and calculations. The total heat transfer to the impingement surface calculated from Eq. 3 was 32 ± 3.0 percent of the fuel input energy. Radiation from the flame to the surroundings was estimated based on a blackbody radiation exchange between the flame and the ambient surroundings. These calculations revealed that the radiation heat transfer from the flame to the surroundings was about 4.0 percent of the fuel input energy supplied to the system. Since the energy convected out of the system and transferred to the surface appear to account for most of the energy available from the fuel input, it can be concluded that radiation from the flame to the surroundings is negligible.

Conclusions

This study was undertaken in order to understand the heat transfer characteristics of a practical RJRC nozzle. Overall heat transfer to the impingement surface depended upon the fuel equivalence ratio, air exit gap width, and fuel Reynolds number. The nozzle-to-plate spacing did not significantly affect the overall heat transfer to the impingement surface. However, for a given nozzle-to-plate spacing, high nozzle centerline flame temperatures were achieved, and the maximum flame temperature and the width of the reaction zone both increased with decreasing distance, H/R_o, from the impingement surface.

Impingement surface heat flux was very high in the reattachment region, while the area averaged heat flux profile identified the possible optimal spacing for future use of RJRC nozzles in array configurations. The relative sizes of the RJRC reaction envelope, high temperature reaction zone, and the reattachment zone were also determined. Calculations revealed the radiation from the flame to the surroundings to be negligible. As a result, the fuel energy was either transferred to the impingement surface or convected out in the combustion product gases. In summary, this study provided the first detailed information regarding the heat transfer characteristics of the RJRC nozzle.

Acknowledgment

This research is partially supported by the Texas Hazardous Waste Research Center and the Texas A&M Drying Research Center. The authors wish to thank Mr. Kai Freudenreich for assistance with the flame temperature measurements.

References

Baukal, C. E., and Gebhart, B., 1995a, "A Review of Flame Impingement Heat Transfer Studies Part 1: Experimental Conditions," *Combustion Science and Technology*, Vol. 104, pp. 339–357.

Baukal, C. E., and Gebhart, B., 1995b, "A Review of Flame Impingement Heat Transfer Studies Part 2: Measurements," *Combustion Science and Technology*, Vol. 104, pp. 359–385.

Boyer, L. M., 1990, "Scalar Dissipation Temperature Measurements in a Lifted Turbulent Diffusion Flame," M.S. Thesis, Brigham Young University, Provo, UT.

Box, G. E. P., and Behnken, D. W., 1960, "Some New Three Level Designs for the Study of Quantitative Variables," *Technometrics*, Vol. 2, No. 4, pp. 455–475.

Bradley, D., and Matthews, K. J., 1968, "Measurement of High Gas Temperatures With Fine Wire Thermocouples," *Journal of Mechanical Engineering Science,* Vol. 10, No. 4., pp. 299–305.

Glassman, I., 1987, *Combustion,* 2nd ed., Academic Press, Inc., Orlando, FL.

Habetz, D. K., Page, R. H., and Seyed-Yagoobi, J., 1994, "Impingement Heat Transfer from a Radial Jet Reattachment Flame," *Proceedings of the 10th International Heat Transfer Conference,* Brighton, England, Vol. 6, pp. 31–36.

Hogg, R. V., and Ledolter, J., 1992, *Applied Statistics for Engineers and Physical Scientists,* Macmillan Publishing Company, New York, NY.

Junus, R., Stubington, J. F., and Sergeant, G. D., 1994, "The Effects of Design Factors on Emissions From Natural Gas Cooktop Burners," *International Journal of Environmental Studies,* Vol. 45, pp. 101–121.

Kline, S. J., and McClintock, F. A., 1953, "Describing Uncertainties in Single Sample Experiments," *Mechanical Engineering,* Vol. 75, pp. 3–8.

Milson, A., and Chigier, N. A., 1973, "Studies of Methane and Methane-Air Flames Impinging on a Cold Plate," *Combustion and Flame,* Vol. 21, pp. 575–586.

Mohr, J. W., 1996, "Studies of Single and Multiple Impinging Radial Jet Reattachment Flames," Ph.D. Thesis, Texas A&M University, College Station, TX.

Mohr, J. W., Seyed-Yagoobi, J., and Page, R. H., 1995, "Optimization of a Practical Radial Jet Reattachment Flame," ASME HTD-Vol. 2, *30th ASME National Heat Transfer Conference,* Portland, OR, pp. 3–10.

Mohr, J. W., Seyed-Yagoobi, J., and Page, R. H., 1996, "Combustion Measurements from an Impinging Radial Jet Reattachment Flame," *Combustion and Flame,* Vol. 106, No. 1–2, pp. 69–80.

Page, R. H., Hadden, L. L., and Ostowari, C., 1989, "Theory for Radial Jet Reattachment Flow," *AIAA Journal,* Vol. 27, No. 11, pp. 1500–1505.

Rigby, J. R., and Webb, B. W., 1995, "An Experimental Investigation of Diffusion Flame Jet Impingement Heat Transfer," *Proceedings of the ASME/JSME Thermal Engineering Joint Conference,* Maui, HI, Vol. 3, pp. 117–126.

Røkke, N. A., Hustad, J. E., and Sønju, O. K., 1994, "A Study of Partially Premixed Unconfined Propane Flames," *Combustion and Flame,* Vol. 97, pp. 88–106.

Turns, S. R., and Lovett, J. A., 1989, "Measurements of Oxides of Nitrogen Emissions from Turbulent Propane Jet Diffusion Flames," *Combustion Science and Technology,* Vol. 66, pp. 233–249.

Viskanta, R., 1993, "Heat Transfer to Impinging Isothermal Gas and Flame Jets," *Experimental Thermal and Fluid Science,* Vol. 6, pp. 111–134.